Surface-Initiated Mechanism for the Formation of Relief Gratings on Azo-Polymer Films

Nirmal K. Viswanathan,[†] Srinivasan Balasubramanian,[‡] Lian Li,[†] Jayant Kumar,[†] and Sukant K. Tripathy*,[‡]

Center for Advanced Materials, Department of Physics and Department of Chemistry, University of Massachusetts at Lowell, Lowell, Massachusetts 01854

Received: March 10, 1998

We report here a detailed experimental study, establishing the surface-initiated mechanism for the photoinduced relief grating formation on azobenzene functionalized polymer films. The grating formation process is found to be strongly dependent on the nature of the surface (20−200 Å), while the birefringent grating appears to be a purely bulk process. Restriction of the surface of the azobenzene polymer film through the deposition of ultrathin top layers of transparent polyelectrolytes by electrostatic self-assembly dramatically decreases the relief grating formation. Thicker polyelectrolyte multilayer film (250 Å) on the surface resulted in the formation of purely birefringent grating, without any surface features.

Introduction

It has been demonstrated that azobenzene functionalized polymers have potential applications in optical data storage,[1,2] electrooptic modulation,[3,4] and direct formation of surface relief gratings (SRG).[5−8] Of particular importance are the SRG's produced on thin films of these materials by irradiating an interference pattern from coherent superposition of laser light of appropriate wavelength. Approaches to their unique application possibilities are only recently being explored.[9−11] For example, subwavelength gratings[12] in these materials may be of significant importance in fabricating efficient waveplates and antireflection surfaces for the visible region. The major advantages of this photofabrication approach are (1) facile one-step processing, (2) large surface modulations obtained at relatively low light intensity levels of a few mW/cm^2, (3) precisely controlled modulation depths by adjusting the exposure energy (J/cm^2), and (4) elimination of contact and wet processing.

Other intriguing features of this surface fabrication technique include strong polarization dependence of both the writing[13] and erasing processes.[14] It is well-known that azo chromophores undergo photoinduced trans ⇒ cis ⇒ trans isomerization, leading to a change in their orientation with respect to the incident polarization.[15] Polarization dependence of writing and erasure of bulk birefringent gratings have been well-defined and understood in terms of the reorientation of the azobenzene chromophores irradiated by polarized light.[16] In this context, it is tempting to account for the relief grating formation, where large-scale photoinduced movement of azobenzene chromophore tethered macromolecules occurs, to this bulk reorientation process and polymer segmental motion arising from associated free volume changes.[17] Barrett et al.[18] formulated a mechanism for the formation of large-amplitude surface deformation in azo-polymer films due to spatially varying volume changes in the bulk.

Efficient photoisomerization clearly "plasticizes" and enhances the mobility of azo-functionalized polymeric material.[19] However, we believe that the SRG recording process as opposed to the birefringent grating process is not a bulk phenomenon and needs an unrestricted surface allowing the movement of polymer chains at the surface. Recently, we have proposed a gradient force model[20] based on the dipolar interaction of the azo-chromophores with the optically induced electric field gradient, leading to macroscopic movement of polymeric material and hence the grating formation. This polymer transport process may be initiated at the film surface and continues through the bulk of the material as polymer layers are moved, leading to high modulation depth gratings.

Experimental verification of the surface-initiated grating formation process is made possible by restricting the free surface of the azo-polymer film. Our earlier experiments revealed that an approximately 1000 Å thick poly(vinyl alcohol) (PVA) film spin-coated on top of the azo-polymer film completely restricted the surface grating formation while birefringent gratings could still be fabricated.[21] However, the thickness of the PVA film was of the order of magnitude of the azo-polymer film and could not be precisely controlled. To firmly establish the role of the surface layers in the deformation process, a more systematic study is necessitated with well-defined ultrathin overlayers on the surface. This opportunity is afforded by a recently reported novel technique of forming ultrathin polymer layers through an alternate layer-by-layer electrostatic deposition of oppositely charged polyelectrolytes.[22−24] This approach has the advantage of controlling layer thickness and organization at the molecular level. This assembly technique has been firmly established for polyelectrolytes[25] and successfully extended to a wide variety of materials such as organic and polymeric microcrystals,[26] organic dyes,[27] ceramics and clay,[28] proteins,[29] and enzymes[30] among others. In this paper, we extend the use of this technique to build constraining molecular layers in a well-defined and controlled manner, by depositing appropriate polyelectrolyte pairs on top of spin-coated azo-polymer film substrates. The grating formation process is monitored by diffracting a He−Ne laser beam and investigating the topography by atomic force microscopy. Photodriven surface deformation process parameters are investigated as a function of the overlayer thickness and composition and found to be dramatically influenced by as

[†] Department of Physics.
[‡] Department of Chemistry.

S1089-5647(98)01425-4 CCC: $15.00
Published on Web 07/10/1998

POLYELECTROLYTES:

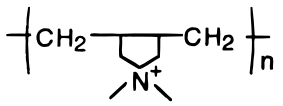

Poly (diallyldimethylammonium chloride)
PDAC.

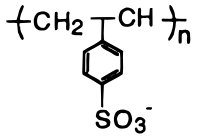

Sulfonated polystyrene
SPS.

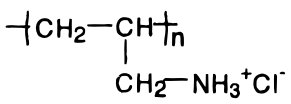

Polyallylamine hydrochloride
PAH.

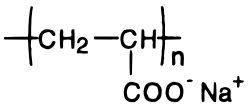

Poly acrylic acid
PAA

AZO POLYMERS:

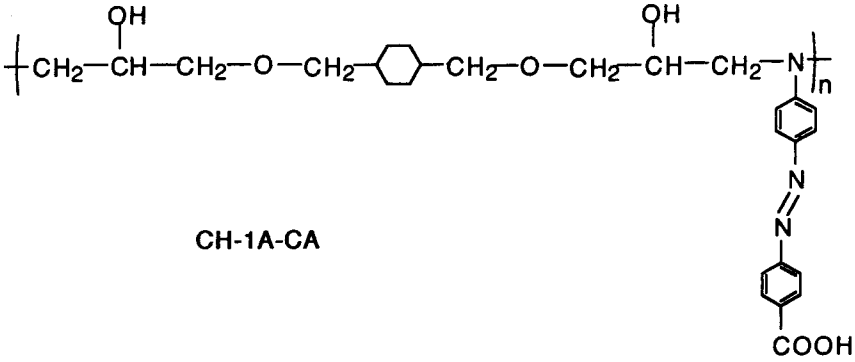

CH-1A-CA

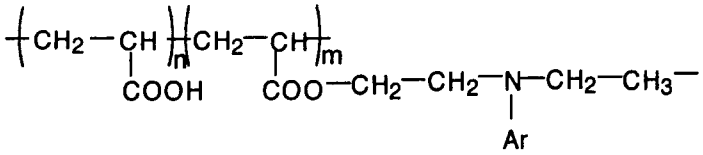

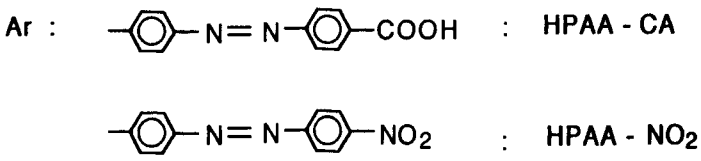

Figure 1. (a, upper) Structures of polyelectrolytes. (b, lower) Structures of azobenzene functionalized polymers.

few as three bilayers (40 Å). The restraining influence of the ultrathin film overlayers is found independent of the azo-polymer itself and the polyelectrolyte pairs.

Experimental Details

Polyelectrolytes. Multilayers of controlled thickness are formed on top of the spin-coated azo-polymer (with free acid groups) films through a sequential layer-by-layer deposition of polycations and polyanions. The detailed methodology for polyelectrolyte-based multilayer self-assembly process is extensively reported.[22−25] The two combinations of polycations and polyanions used in this study are poly(diallyldimethylammonium chloride) PDAC:sulfonated polystyrene SPS and poly(allylamine hydrochloride) PAH:poly(acrylic acid) PAA. The structures of these medium molecular weight polyelectrolytes (purchased from Aldrich) are given in Figure 1a. Each of these polyelectrolytes is dissolved in 30 mL of Milli-Q water at 10 mM concentration and its pH is adjusted to be 3.0 ± 0.1. The azo-polymer film substrate is first kept dipped into the polycation solution for about 10 min. During this time, a monolayer of the polycation is adsorbed through electrostatic interaction. The film is rinsed with pH-adjusted Milli-Q water (pH = 3.0 ± 0.1) and dipped into the polyanion solution for an equal amount of time and is subsequently rinsed again. This process adsorbs one bilayer of controlled thickness on the azo-polymer substrate and is repeated to form multilayers. As the film quality, uniformity of the spread, and the thickness of the multilayers depend on solution concentration and pH values, the solutions are constantly replenished, and their pH values are monitored after every five dippings. Observing the films under an optical microscope clearly shows a uniform spread of the overlayer coating without any damage to the azo-polymer film substrate.

In a typical experiment, to monitor the thickness of the multilayer formation on the azo-polymer substrate, a precleaned, hydrolyzed glass slide is dipped alongside. The assumption made here is that, after the initial few bilayers (1−3), the multilayer formation is independent of the nature of the substrate

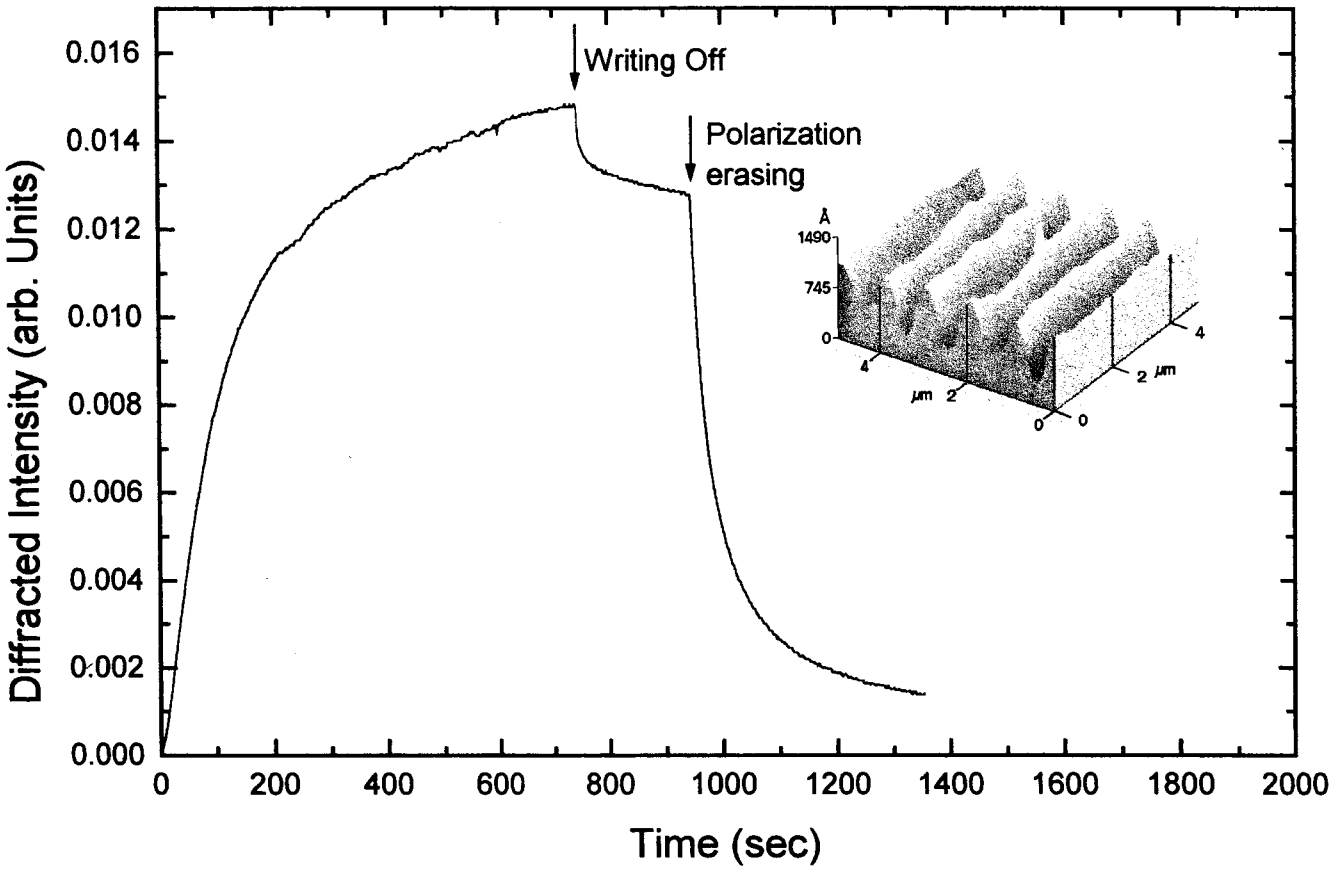

Figure 2. Diffracted intensity monitored as a function of time during the photofabrication and photoerasure of SRG in high molecular weight HPAA-CA azo-polymer. Inset shows a typical AFM image of the SRG.

and continues to form the same way as long as there is enough surface charge density. The glass substrate is removed after every five bilayers and is dried with a jet of nitrogen to measure the absorption and thickness. The UV−vis absorption spectra of the bilayers formed, measured using a Perkin-Elmer, Lambda-9 spectrophotometer, show increase in absorption with respect to the number of bilayers. The thickness of the multilayer films formed on the glass slides is measured using an AutoEL-III automatic ellipsometer (Rudolph Research) with a He−Ne laser.

Azo-Polymers. The azobenzene functionalized polymers used in this study are selected from two polymer backbone classes. The different main chain and side chain groups of the polymers offer different sites for electrostatic attachment of polyelectrolytes. Chemical structures of the three azo-polymers CH-1A-CA, HPAA-CA, and HPAA-NO_2 are given in Figure 1b. These azo-functionalized polymers are synthesized by a versatile post-azo coupling reaction.[31,32] CH-1A-CA is derived from epoxy-based water-soluble azo-polymer-containing ionizable groups in the azobenzene functionality. The number-average molecular weight of this polymer is 5000 g/mol, and its T_g is 93 °C. Synthetic details and characterization of the azo-polymer CH-1A-CA are reported elsewhere.[33] The other two azobenzene chromophore functionalized poly(acrylic acid) (PAA) copolymers (HPAA-CA and HPAA-NO_2) were synthesized through modification of the high molecular weight (250 000 g/mol) poly(acrylic acid). Commercially available PAA was partially esterified (50%) with *N*-ethylaniloethanol to yield the anilino functional copolymer. The para position of the aniline moiety can be readily functionalized through a post-azo coupling reaction.[31,32] Upon reaction with the diazonium salt of 4-aminobenzoic acid this polymer resulted in HPAA-CA, and reaction with the diazonium salt of 4-nitroaniline yielded HPAA-NO_2. The average molecular weights increases to about 500 000 on esterification, which increases further on azo functionalization (no GPC evidence because of problems with determination in the high MW range). The polymers are highly soluble in polar organic solvent such as DMF, DMSO, etc., and can be spin-coated into optical quality films. The T_g of the two polymers are 85 and 91 °C, respectively. These side chain azo-polymers were designed to contain ionizable groups in the chromophores, and under appropriate pH conditions, they behave like polyelectrolytes.[34] A 100 mg sample of each azo-polymer is dissolved in 1 mL of DMF and is spin-coated on preprocessed glass slides and vacuum-dried to get good optical quality films. The refractive index and thickness of these films are measured using a prism coupler (Metricon 2010). The average thickness of the spin-coated films is 0.6 μm.

A simple two-beam interferometer setup is used for the formation of surface relief gratings on the spin-coated azo-polymer films.[2,6] A linearly polarized Ar^+ laser beam at 488 nm after passing through a half-wave plate is spatially filtered and collimated and is incident on the sample stage. The sample stage consists of two platforms fixed at right angles. A mirror is attached to one of the platforms, and the polymer sample is fixed to the other. By rotating the sample stage to an angle of 14°, we can write gratings with periodicity of $\Lambda = 1$ μm. The advantages of this simple experimental arrangement have been discussed and demonstrated in earlier publications.[7,35,36] The formation of the relief grating is monitored continuously by diffracting a low-power, unpolarized He−Ne laser at 633 nm in the transmission configuration. The diffracted signal intensity (+1 order) is recorded as a function of time. The half-wave

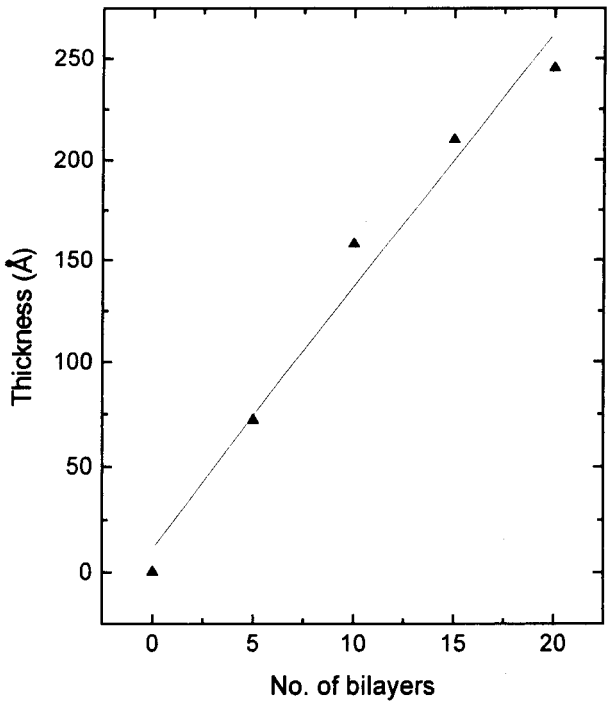

Figure 3. Thickness vs number of bilayers of PDAC:SPS polyelectrolytes on a glass substrate.

plate is rotated to get a $\alpha = 45°$ polarized light which is shown to inscribe high modulation depth relief gratings.[13] The intensity of the recording laser beam monitored after the collimator lens is kept fixed at 50 mW/cm^2 for all our recordings. Surface topography of the relief gratings is probed using an atomic force microscope (AFM, Cp, Park Scientific, Sunnyvale, CA). The AFM was operated in the contact mode using a SiN cantilever. All the gratings recorded are imaged by 5 μm $\times$ 5 μm scans at 1 Hz rate at three different places.

Results and Discussion

Efficient SRG formation in the epoxy-based low molecular weight CH-1A-CA azo-polymer films has already been demonstrated by our group.[37] The grating formation behavior in the very high molecular weight poly(acrylic acid)-based polymer films monitored through the diffracted beam intensity is found to be surprisingly similar, although somewhat less efficient, to that observed earlier for low molecular weight azo-polymer films. Figure 2 shows the formation of SRG and the subsequent optical erasure in the high molecular weight HPAA-CA azo-polymer. The maximum efficiency measured in the +1 order of the diffracted beam is about 8%. When the writing laser beam is turned off, the initial decrease in the diffracted beam intensity is due to the decay of the orientation grating. The subsequent erasing process of the grating using a single, 45° polarized beam shows an almost complete decay of the diffracted beam intensity and no clear surface features in an AFM scan. The inset in the figure is an AFM image of the grating scanned at the end of "writing off". The modulation depth of the SRG formed in this material is 745 Å. The large number of entanglements expected in high molecular weight polymers such as HPAA-CA is possibly the reason for less efficient SRG formation.

Polyion multilayer is formed on the azo-polymer substrates in such a way that they cover only half of the substrate. The thickness of the PDAC:SPS multilayer deposited on the frosted glass slides (used as control) was determined using an ellipsometer. The thickness of each adsorbed individual polyion layer depends mainly on the pH of the dipping solution.[37] In our case, the determining criteria for optimum pH values of the polyelectrolyte solutions are the quality of the multilayer films and their controlled thickness (as thin as possible with uniform coverage) that can be formed on top of the spin-coated azo-polymer film. In addition, it was found that, at pH values higher than 3.0, the azo-polymer film (in this case itself a polyacid) gets affected to different extent during the initial dipping into these solutions. A plot of thickness versus the number of bilayers (Figure 3) formed at pH 3 shows an almost linear increase. The slope of the straight line gives the average thickness per bilayer to be 12.5 Å. The thickness per bilayer of the polyelectrolytes deposited on top of the azo-polymer film can be reasonably assumed to be within ±10% of this value. These polyion bilayers are expected only to restrict the surface-initiated material movement and hence the grating formation due to their electrostatic attachment with the azo-polymer film substrate.

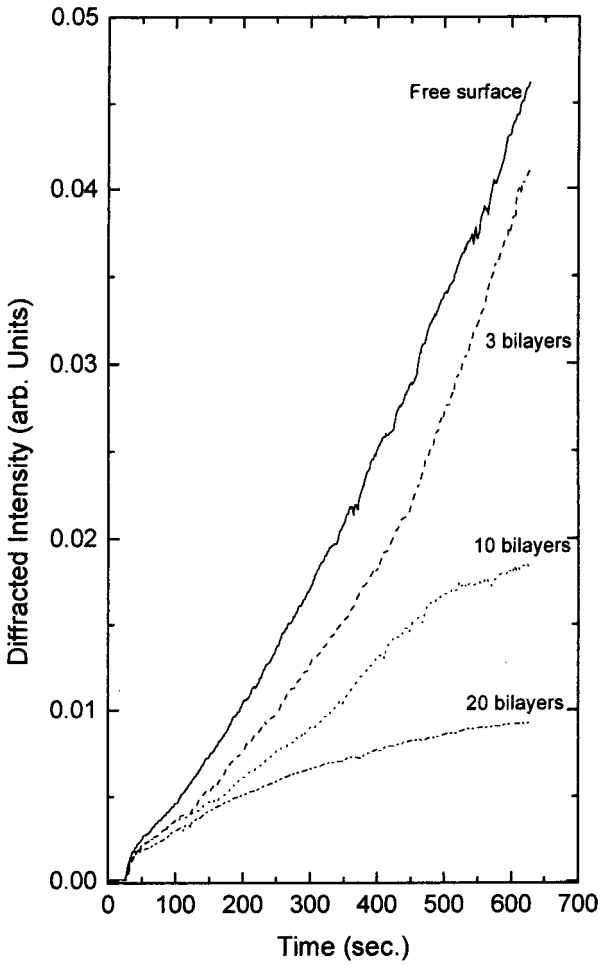

Figure 4. Diffracted intensity as a function of time measured for unrestricted CH-1A-CA azo-polymer and with different number of overlaid bilayers of PDAC:SPS.

The interference pattern formed due to coherent superposition of the Ar^+ laser beam is incident overlapping both the uncovered (free surface) and multilayer overlaid portions of the azo-polymer film. This enables us to monitor the effect of restricting the free surface on the surface relief grating formation process of the azo-polymer film. Figure 4 gives a plot of the time evolution of the grating formation on the unrestricted CH-1A-CA azo-polymer and with 3, 10, and 20 bilayers of PDAC:SPS overlaid portions. The diffracted intensity from the grating

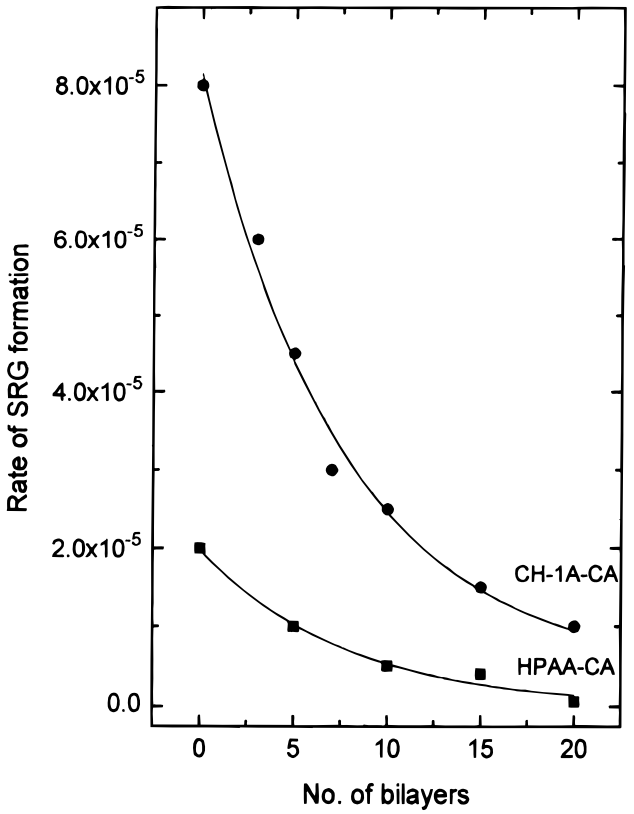

Figure 5. Rate of surface relief grating formation plotted as a function of the number of bilayers for CH-1A-CA and HPAA-CA azo-polymers with multilayer coatings of PDAC:SPS and PAH:PAA, respectively.

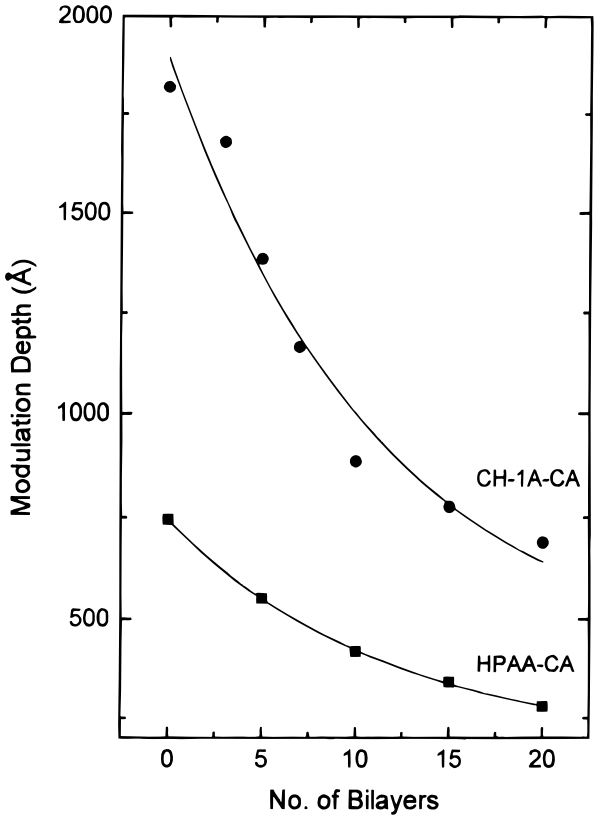

Figure 6. Plot of modulation depth of the surface relief grating measured using AFM as a function of number of bilayers for CH-1A-CA and HPAA-CA azo-polymers with overlaid multilayer coatings of PDAC:SPS and PAH:PAA, respectively.

written for 11 min for the uncovered portion shows the already established behavior.[7,13] The initial increase in the diffracted intensity during the first few tens of seconds is known to be predominantly due to the contribution from the preferential orientation of the azo-chromophores in the bulk resulting in a birefringence grating and shows no surface features in an AFM scan.[7,13] As exposure to the interference pattern is continued, light-induced forces acting on the polymer chains initiate the mass transport at the surface leading to the appearance of surface modulation. As time progresses, diffraction efficiency continues to increase almost linearly with exposure until fairly high surface modulation is achieved. It has been established that the evolution of the surface relief grating at this intensity (50 mW/cm^2) and time scale is dose dependent.[36]

The grating formation process in the region overlaid with ultrathin multilayer shows a drastically different behavior with increase in the number of bilayers (Figure 4). The transparent multilayer of PDAC:SPS formed on the CH-1A-CA azo-polymer substrate is expected to restrict the free movement of the macromolecules on the azo-polymer−PDAC interface. However, trans ⇒ cis ⇒ trans photoisomerization in the bulk and other photoinduced bulk processes are unimpeded. Dramatic decrease in the rate of the surface grating formation process leading to a decrease in the maximum value of the diffracted intensity is observed for the same dose level. For 10 and higher number of bilayer overlaid films, after an initial increase, the diffracted intensity tends to saturate. Even a three bilayer (40 Å, maximum) overlayer on top of the azo-polymer film considerably slows the grating formation rate. After 400 s of exposure, the writing rate appears to increase for this film (as opposed to leveling off for the 10- and 20-bilayer overlaid film) analogous to the free surface azo-polymer film. This interesting behavior may be understood in light of possible disruption of the overlaid multilayer film as surface topography begins to change and as significant energies are dissipated at the interface. At short writing times (below 400 s), however, even this thin an overlaid film has effectively restricted the surface deformation process.

To further verify the consistency of the results and to make sure that the grating formation process is dependent on the nature of the surface, the experiments were repeated with all the three different azo-polymers and both sets of polyion pairs. The actual reduction in the grating efficiency can be determined from the linear portion of the plot of the diffracted intensity versus time and from the measured modulation depth of the gratings. The portion from where the surface grating formation process is expected to begin (after initial 3−4 min) is fitted to a straight line. The slope of the straight line gives the rate of formation of the surface relief grating on the unrestricted azo-polymer and with different number of bilayers. Figure 5 shows that the SRG formation rate decreases exponentially with the number of bilayers for both CH-1A-CA and HPAA-CA azo-polymers, indicating the effect of constrained surface during the grating formation process. As expected, the thicker the overlaid film, the more difficult it is to move the materials that are electrostatically tied to the polyion, and hence there is a decrease in the formation rate of the grating as observed through the diffracted beam. However, a 250 Å thick transparent polymer on top seems to almost completely inhibit the grating formation process on the azo-polymer film.

The decrease in the grating formation process with overlayers is further confirmed by the modulation depth measurement using the AFM. The average modulation depth of the sinusoidal gratings written for 30 min on unrestricted CH-1A-CA azo-polymer is 1820 Å, corresponding to a diffraction efficiency of

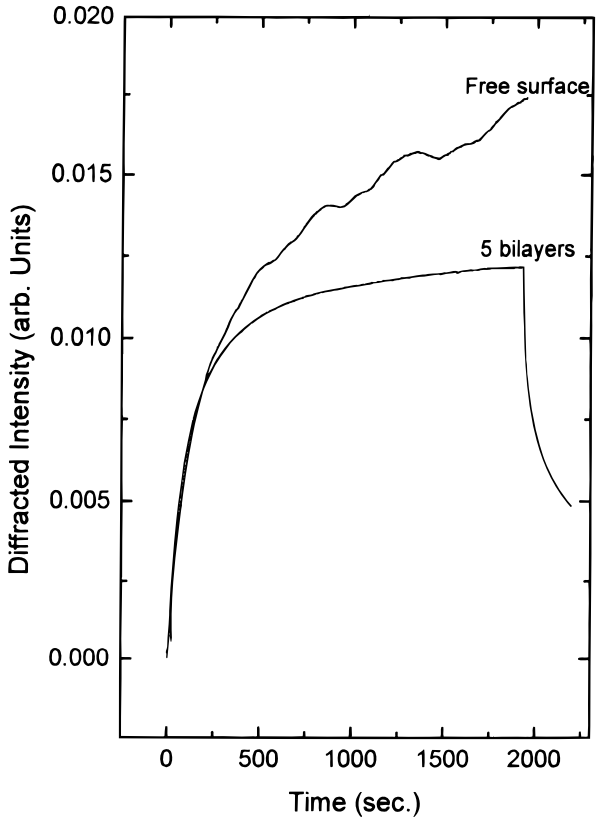

Figure 7. Diffracted intensity as a function of time for the unrestricted HPAA-NO_2 azo-polymer and with five overlaid bilayers of PAH:PAA.

18% in the +1 diffraction order. As the number of bilayers of PDAC:SPS formed on top of the azo-polymer is increased, the modulation depth shows an exponential decrease as shown in Figure 6. We have also performed these measurements for the HPAA-CA azo-polymer and PAH:PAA polyions, and the behavior appears similar to the other azo-polymeric materials, polyion combination. By comparing the characteristic behavior of SRG formation without and with restricting multilayers given in Figures 5 and 6, it is clear that it takes thicker multilayers to inhibit the SRG formation in more efficient materials such as CH-1A-CA than in high molecular weight and less efficient polymers such as HPAA-CA.

By restricting the surface of the high molecular weight azo-polymer HPAA-NO_2 with relatively thinner bilayers, we were able to completely stop the surface-initiated grating formation. In this material, the surface gratings formed are less efficient compared with the ones formed in the other two azo-polymers (Figure 7). The reason is attributed mainly to the high molecular weight of the polymer material. The modulation depth of the SRG written for 30 min measured by AFM is 220 Å, which corresponds to a diffraction efficiency of less than 2%. After forming five bilayers (75 Å, maximum) of PAH:PAA on top of the thin film of HPAA-NO_2, the experiment is repeated. The diffraction efficiency initially shows an increase but remains constant at that level until the end of the recording. This saturated behavior of the diffracted intensity is attributed mainly to the bulk orientation grating formed in this material. The diffraction efficiency from the bulk birefringence grating increases until a photostationary equilibrium is reached and remains constant because the surface of the azo-polymer is restricted from free movement. Our argument of predominant birefringent grating in this case is confirmed by turning off the writing laser beam and continuing to monitor the diffracted beam. The diffracted signal is seen to decrease to about 60% of the maximum value in just a few minutes (Figure 7). This indicates that some of the chromophores randomize their orientation once the aligning optical field is removed. Furthermore, an AFM scan of the irradiated region shows no appearance of any surface features, confirming the formation of only bulk orientation grating.

Conclusions

Photofabrication and effective photoerasure of surface relief gratings in high molecular weight azobenzene functionalized polymers of HPAA-CA and HPAA-NO_2 are demonstrated for the first time. Large-scale molecular migration of polymer chains at the surface of the azo-polymer films initiated by appropriate photoexcitation of the azo-chromophores appears to be responsible for this process. Photoplasticization through efficient trans ⇒ cis isomerization of the azo-chromophores at the polymer surface along with the photodriven transport leads to the surface relief grating formation. By restricting the surface of azo-polymer films on which gratings are written, in a controlled manner we were able to demonstrate convincingly the necessity for a free, unconstrained surface to form efficient relief gratings. Thicker (≈250 Å**)** overlayers almost completely inhibit the surface-initiated movement of the azo-polymers while predominantly birefringent gratings without any surface features are easily formed.

Acknowledgment. Financial support from ONR-MURI is gratefully acknowledged. Extensive discussions with MURI partners, Prof. Michael F. Rubner at MIT and Prof. Daniel J. Sandman at UMass, Lowell, are acknowledged.

References and Notes

(1) Eich, M.; Wendroff, J. H.; Reck, B.; Ringsdorf, H. *Makromol. Chem. Rapid Commun.* **1987**, *8*, 59.
(2) Xie, S.; Natansohn, A.; Rochon, P. *Macromolecules* **1995**, *28*, 8835.
(3) Sawodny, M.; Schmidt, A.; Stamm, M.; Knoll, W.; Urban C.; Ringsdorf, H. *Polym. Adv. Technol.* **1991**, *2*, 127.
(4) Seki, T.; Skuragi, M.; Kawanishi, Y.; Suzuki, Y.; Tamiki, T.; Fukuda R.; Ichimura, K. *Langmuir* **1993**, *9*, 211.
(5) Rochon, P.; Batalla E.; Natanshon, A. *Appl. Phys. Lett.* **1995**, *66*, 136.
(6) Kim, D. Y.; Li, L.; Kumar, J.; Tripathy, S. K. *Appl. Phys. Lett.* **1995**, *66*, 1166.
(7) Kim, D. Y.; Li, L.; Jiang, X. L.; Shivshankar, V.; Kumar J.; Tripathy, S. K. *Macromolecules* **1995**, *28*, 8835.
(8) Holme, N. C. R.; Nikolova, L.; Ramanujam, P. S.; Hvilsted, S. *Appl. Phys. Lett.* **1997**, *70*, 1518.
(9) Li, L.; Jiang, X. L.; Kim, D. Y.; Kumar, J.; Tripathy, S. K. *Technical Digest*; Optical Society of America: Washington, DC, 1997; Vol. 14, p 214.
(10) Kim, D. Y.; Lee, T. S.; Wang, X.; Jiang, X. L.; Li, L.; Kumar, J.; Tripathy, S. K. *Proc. SPIE* **1997**, *2998*, 195.
(11) Rochon, P.; Natansohn, A.; Callender, C. L.; Robitaille, L. *Appl. Phys. Lett.* **1997**, *71*, 1008.
(12) Raguin, D. H.; Morris, G. M. *Laser Focus World* **1997** (April), 113.
(13) Jiang, X. L.; Li, L.; Kim, D. Y.; Shivshankar, V.; Kumar, J.; Tripathy, S. K. *Appl. Phys. Lett.* **1996**, *68*, 2618.
(14) Jiang, X. L.; Li, L.; Kumar, J.; Kim, D. Y.; Tripathy, S. K. *Appl. Phys. Lett.* **1998**, *72*, 2502.
(15) Todorov, T.; Nikolova, L.; Tomova, N. *Appl. Opt.* **1984**, *23*, 4309; **1984**, *23*, 4588.
(16) Rochon, P.; Gosselin, J.; Natansohn, A.; Xie, S. *Appl. Phys. Lett.* **1992**, *60*, 4.
(17) Eisenbach, C. D. *Ber. Bunsen-Ges. Phys. Chem.* **1980**, *84*, 680.
(18) Barrett, C. J.; Natansohn, A.; Rochon, P. L. *J. Phys. Chem.* **1996**, *100*, 8836.
(19) Bohm, N.; Materny, A.; Keifer, W.; Steins, H.; Muller, M. M.; Schottner, G. *Macromolecules* **1996**, *29*, 2599.
(20) Kumar, J.; Li, L.; Jiang, X. L.; Kim, D. Y.; Lee, T. S.; Tripathy, S. K. *Appl. Phys. Lett.* **1998**, *72*, 2096.
(21) Tripathy, S. K.; Kim, D. Y.; Jiang, X. L.; Li, L.; Lee, T. S.; Wang, X.; Kumar, J., to be published in *Mol. Cryst. Liq. Cryst.*
(22) Decher, G.; Hong, J. D. *Makromol. Chem., Macromol. Symp.* **1991**, *46*, 321.

(23) Decher, G.; Hong, J. D.; Schmitt, J. *Thin Solid Films* **1992**, *210/211*, 831.
(24) Ferreira, M.; Cheung, J. H.; Rubner, M. F. *Thin Solid Films* **1994**, *244*, 806.
(25) Decher, G. *Science* **1997**, *277*, 1232.
(26) Tripathy, S. K.; Katagi, H.; Kasai, H.; Balasubramanian, S.; Oshikiri, H.; Kumar, J.; Oikawa, H.; Okada, S.; Nakanishi, H. *Jpn. J. Appl. Phys.* **1998**, *37*, L343.
(27) Ariga, K.; Lvov, Y.; Kunitake, T. *J. Am. Chem. Soc.* **1997**, *119*, 2224.
(28) Lvov, Y.; Ariga, K.; Ichinose, I.; Kunitake, T. *Langmuir* **1996**, *12*, 3038.
(29) Caruso, F.; Niikura, K.; Furlong, D. N.; Okahata, Y. *Langmuir* **1997**, *13*, 3427.
(30) Onada, M.; Lvov, Y.; Ariga, K.; Kunitake, T. *Biotechnol. Bioeng.* **1996**, *51*, 163.
(31) Wang, X.; Li, L.; Chen, J.; Marturunkakul, S.; Kumar, J.; Tripathy, S. K. *Chem. Mater.* **1997**, *9*, 45.
(32) Wang, X.; Li, L.; Chen, J.; Marturunkakul, S.; Kumar, J.; Tripathy, S. K. *Macromolecules* **1997**, *30*, 219.
(33) Wang, X.; Balasubramanian, S.; Li, L.; Jiang, X. L.; Sandman, D. J.; Rubner, M. F.; Kumar, J.; Tripathy, S. K. *Macromol. Rapid Commun.* **1997**, *18*, 451.
(34) Balasubramanian, S.; Wang, X.; Wang, H. C.; Yang, K.; Kumar, J.; Tripathy, S. K. *Chem. Mater.* **1998**, *10*, 1554.
(35) Rochon, P.; Mao, J.; Natansohn, A.; Batalla, E. *Polym. Prepr. (Am. Chem. Soc., Polym. Chem.)* **1994**, *35* (2), 154.
(36) Mai, X.; Moshrefzadeh, R. S.; Gibson, U. J.; Stegeman, G. I.; Seaton, C. T. *Appl. Opt.* **1985**, *24*, 3155.
(37) Tripathy, S. K.; Kim, D. Y.; Kumar, J.; Li, L.; Xiang, X. L. *Naval Res. Rev.* **1997**, *XLIX*, 31.
(38) Decher, G.; Schmitt, J. *Prog. Colloid Polym. Sci.* **1992**, *89*, 160.